

Nucleic acid recognition by Toll-like receptors is coupled to stepwise processing by cathepsins and asparagine endopeptidase

Sarah E. Ewald,¹ Alex Engel,¹ Jiyoun Lee,^{2,3} Miqi Wang,¹
Matthew Bogyo,^{2,3} and Gregory M. Barton¹

¹Division of Immunology and Pathogenesis, Department of Molecular and Cell Biology, University of California, Berkeley, Berkeley, CA 94720

²Department of Pathology and ³Department of Microbiology and Immunology, Stanford University School of Medicine, Stanford, CA 94305

Toll-like receptor (TLR) 9 requires proteolytic processing in the endolysosome to initiate signaling in response to DNA. However, recent studies conflict as to which proteases are required for receptor cleavage. We show that TLR9 proteolysis is a multistep process. The first step removes the majority of the ectodomain and can be performed by asparagine endopeptidase (AEP) or cathepsin family members. This initial cleavage event is followed by a trimming event that is solely cathepsin mediated and required for optimal receptor signaling. This dual requirement for AEP and cathepsins is observed in all cell types that we have analyzed, including mouse macrophages and dendritic cells. In addition, we show that TLR7 and TLR3 are processed in an analogous manner. These results define the core proteolytic steps required for TLR9 function and suggest that receptor proteolysis may represent a general regulatory strategy for all TLRs involved in nucleic acid recognition.

CORRESPONDENCE
Gregory M. Barton:
barton@berkeley.edu

Abbreviations used: AEP, asparagine endopeptidase; endo H, endoglycosidase H; LI-1, legumain inhibitor; LRR, leucine-rich repeat; MEF, mouse embryonic fibroblast; TLR, toll-like receptor.

Toll-like receptors (TLRs) are a family of pattern recognition receptors that have evolved to detect invading microorganisms and link recognition to induction of antimicrobial defense. In mammals, TLR9, TLR7, and TLR3 recognize nonmethylated CpG motifs in DNA, single-stranded RNA, and double-stranded RNA, respectively. These ligands are conceptually distinct among TLRs because they exist within the host as well as within potential pathogens. Thus, although nucleic acid recognition enables detection of viral infection, this strategy can also result in self-recognition. Indeed, recognition of self–nucleic acids by TLR7 and TLR9 can contribute to the pathology of autoimmune diseases such as rheumatoid arthritis and systemic lupus erythematosus (Krieg and Vollmer, 2007). These observations indicate that, unlike other TLR family members, the ability to distinguish between self- and nonself–nucleic acids is not based simply on molecular recognition. Instead, the capacity to bind nucleic acids has been coupled to a unique localization and regulatory program, which appears to play an important role in limiting the potential for self–nucleic acid recognition (Barton et al., 2006).

TLR3, TLR7, and TLR9 localize to and exclusively signal from endolysosomal compartments. Unlike the surface-localized TLRs, these TLRs have an ER-resident pool, and exit from the ER is controlled by Unc93b1 (Tabeta et al., 2006; Ewald et al., 2008; Kim et al., 2008). Perhaps most strikingly, recent studies have demonstrated that TLR9 is processed in endolysosomal compartments by resident proteases and this processing is required to generate a functional receptor (Ewald et al., 2008; Park et al., 2008; Sepulveda et al., 2009).

Although there is consensus that acid-dependent proteases are required for TLR9 processing, the specific proteases involved remain somewhat controversial (Ewald et al., 2008; Park et al., 2008; Sepulveda et al., 2009). Cathepsins are likely candidates, as members of this protease family are activated in a pH-dependent manner throughout endosome maturation and play a well established role in peptide processing

© 2011 Ewald et al. This article is distributed under the terms of an Attribution-Noncommercial-Share Alike-No Mirror Sites license for the first six months after the publication date (see <http://www.upress.org/terms>). After six months it is available under a Creative Commons License (Attribution-Noncommercial-Share Alike 3.0 Unported license, as described at <http://creativecommons.org/licenses/by-nc-sa/3.0/>).

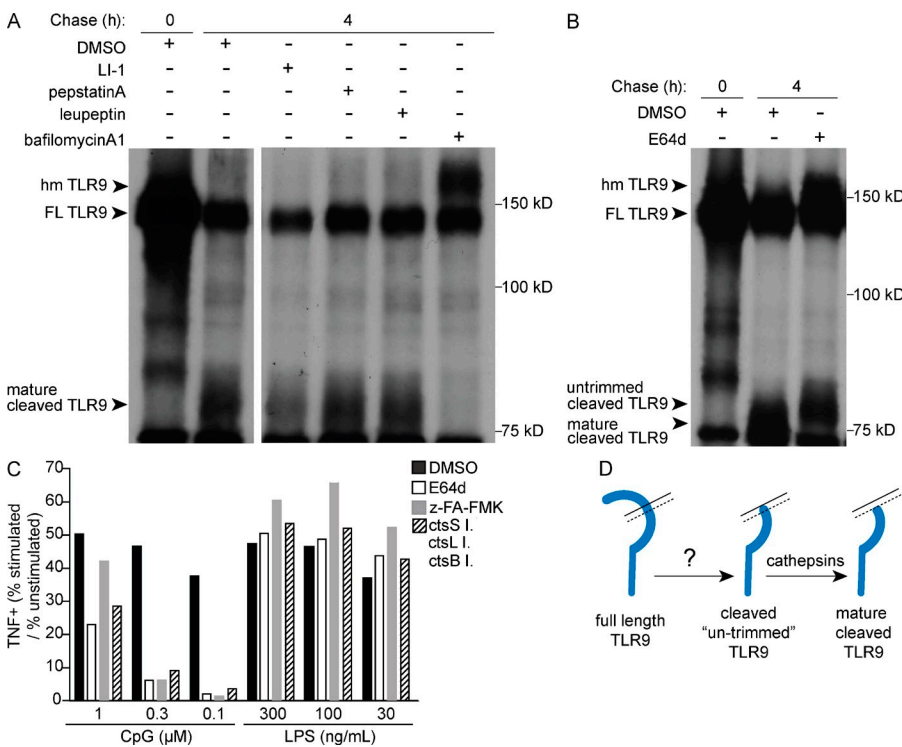


Figure 1. TLR9 cleavage is a multistep event. (A and B) TLR9 cleavage in TLR9-RAW cells was monitored by pulse-chase analysis in the presence of the indicated protease inhibitors or DMSO (as vehicle control). The full-length form of TLR9 (FL TLR9) and two cleavage products (mature cleaved TLR9 and untrimmed cleaved TLR9) are labeled. The pool of full-length TLR9 that has exited the ER but has not yet been cleaved is also labeled (hm TLR9). (C) Analysis of TNF production by intracellular cytokine staining. RAW cells were pretreated for 12 h with the indicated protease inhibitors (broad spectrum cathepsin inhibitor [z-FA-FMK or E64d], AEP inhibitor [LI-1], a combination of ctsS inhibitor [ctsS I.], ctsL inhibitor [ctsL I.], and ctsB inhibitor [ctsB I.], or vehicle control [DMSO]) followed by 4 h of stimulation with the indicated concentrations of CpG or LPS. Graph represents the ratio of the percentage of TNF-expressing cells in stimulated and unstimulated conditions. Representative FACS plots are shown in Fig. S2. (D) Schematic depicting the unique requirement of cathepsins for trimming TLR9 once the majority of the ectodomain has been removed, generating the mature form of the cleaved receptor. All data are representative of at least five experiments.

for MHCII loading in macrophage and DCs (Rudensky and Beers, 2006). Before the discovery of TLR9 proteolysis, ctsB and ctsL, as well as ctsK, were implicated in TLR9 signaling in studies using Baf/3 cells and an antigen-induced arthritis model, respectively (Asagiri et al., 2008; Matsumoto et al., 2008). However, the use of knockout mice has ruled out ctsB, ctsL, ctsK, ctsS, and ctsF as individual proteases required for TLR9 processing in macrophages (Ewald et al., 2008; Park et al., 2008). One study noted that combined treatment with ctsS and ctsL inhibitors resulted in a larger nonfunctional form of cleaved TLR9, dubbed the “pre-C-terminal fragment,” suggesting that certain cathepsin family members may play a more prevalent role in TLR9 processing than others (Park et al., 2008). However, a recent paper by Sepulveda et al. (2009) has shown that asparagine endopeptidase (AEP; also known as mammalian legumain), a cysteine protease with a strict substrate specificity for asparagine residues, is required for TLR9 processing and signaling in DCs. Under resting conditions, AEP-deficient cells were unable to cleave phagosomal TLR9 and signaling was greatly impaired.

Based on these results, it is unclear how all of these proteases contribute to TLR9 processing and signaling events. TLR9 processing could be achieved by the functionally redundant role of different proteases depending on cell type, or several proteases could perform complementary, nonoverlapping, or partially overlapping roles in the processing of TLR9. Furthermore, the studies discussed in the previous paragraphs have largely focused on TLR9 as a representative of the nucleic acid-sensing TLRs. Recent results conflict as to whether TLR7, which also contributes to autoimmunity, is subject to the same proteolytic regulation as TLR9 (Ewald et al., 2008;

Park et al., 2008).

The question of whether TLR3 is cleaved has not been addressed.

To resolve these outstanding questions, we have examined the role of different proteases in receptor processing in macrophages, DCs, and fibroblasts. We find that receptor cleavage occurs through a multistep process. The first step can be mediated either by AEP or by multiple members of the cathepsin family of proteases. This first processing event is followed by a second, exclusively cathepsin-mediated, N-terminal trimming which is also required for optimal receptor function. These requirements appear to be conserved across all cell types analyzed. Importantly, we also show that TLR7 and TLR3 are processed in a similar manner, implying that receptor proteolysis is a conserved mode of regulating all nucleic acid-sensing TLRs.

RESULTS AND DISCUSSION

Cathepsins mediate secondary trimming of cleaved TLR9

To address the question of which proteases are required for TLR9 processing, we performed a detailed analysis of the effects of various protease inhibitors on RAW cells (a macrophage cell line) stably transduced with a C-terminally HA-tagged version of TLR9 (TLR9-RAW). Treatment with broad-spectrum serine (pepstatin A) or cysteine (leupeptin) inhibitors or with a highly selective aza-peptidyl-asparagine epoxide inhibitor of AEP (or legumain inhibitor 1 [LI-1]; Lee and Bogyo, 2010) did not block TLR9 cleavage (Fig. 1 A). Upon treatment with cathepsin inhibitor E64d (also known as EST; Fig. 1 B) or z-FA-FMK (Fig. 2 A), the majority of the ectodomain was still removed; however, the resulting

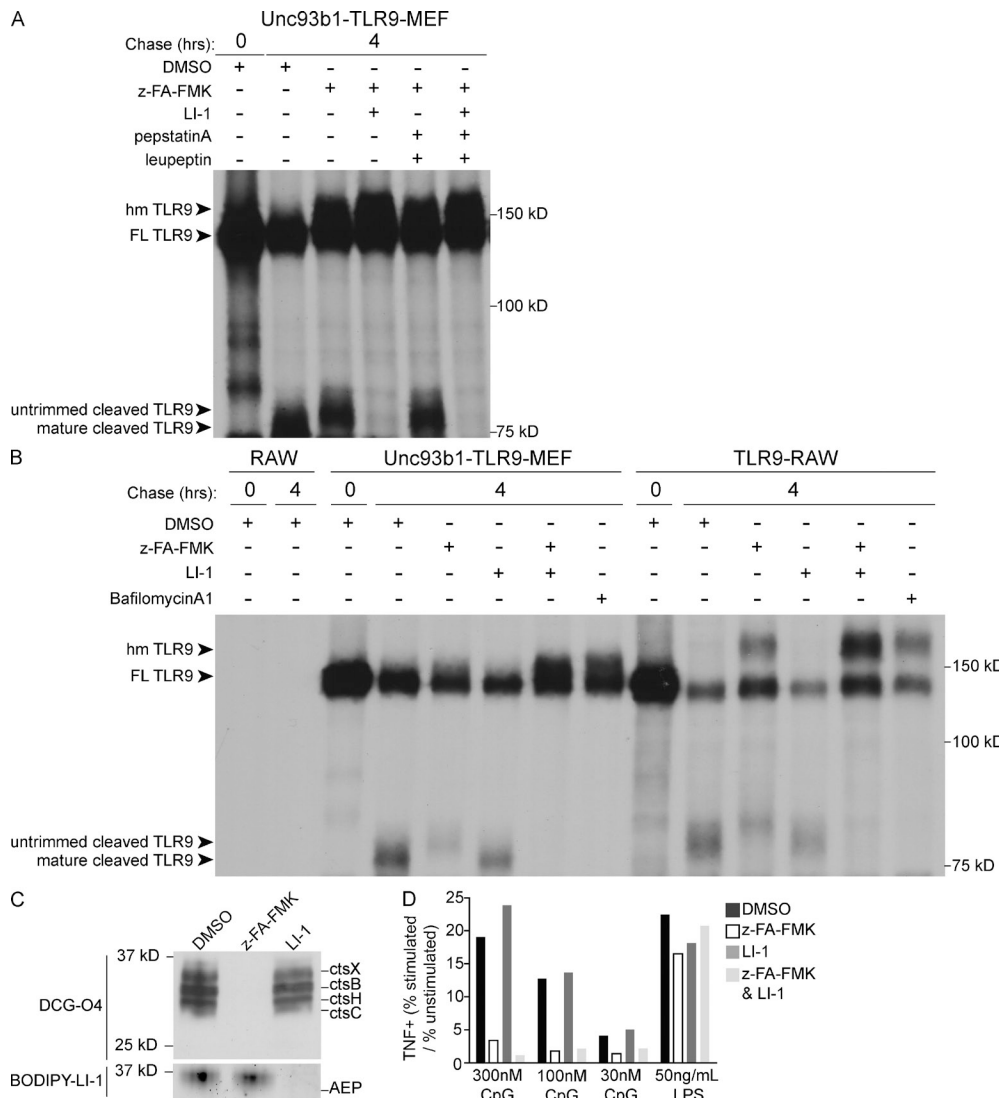


Figure 2. AEP and cathepsins account for cleavage of the TLR9 ectodomain. (A and B) TLR9 cleavage in Unc93b1-TLR9-MEF cells or TLR9-RAW cells was monitored by pulse-chase analysis in the presence of indicated protease inhibitors or DMSO (as vehicle control). (C) Efficiency of protease inhibition of live cells was determined by probing cell lysates with tagged protease inhibitor probes. RAW cells were pretreated with z-FA-FMK (z-FA), LI-1, or DMSO. Cell lysates were then probed with the cathepsin probe DCG-04-biotin (top) or the AEP probe BODIPY-LI-1 (bottom) and visualized as described in Materials and methods. Bands corresponding to individual proteases are indicated on the right. (D) Analysis of TNF production by RAW cells using intracellular cytokine staining as described in Fig. 1. Representative FACS plots are shown in Fig. S3. All data are representative of at least three experiments.

Downloaded from http://jpress.org/jem/article-pdf/208/4/643/1903746/jem_20100682.pdf by guest on 08 February 2026

C-terminal product was slightly larger than that observed in untreated cells (Fig. 1 B). To better resolve this size difference, we used the endoglycosidase PNGase to remove N-linked sugars from the C-terminal TLR9 fragment. Deglycosylation revealed several distinct bands within the C-terminal fragment which otherwise appear as a single diffuse band (Fig. S1). Moreover, in the presence of z-FA-FMK these deglycosylated bands shifted to a higher molecular mass. These data are consistent with the interpretation that cathepsins can trim additional fragments from the TLR9 C terminus after the initial cleavage event (Park et al., 2008). Furthermore, the presence of multiple bands in z-FA-FMK-treated

cells suggests that the initial proteolytic event can occur at multiple sites within TLR9.

In previous work, we established that full-length TLR9 that has exited the ER is modified so that it appears to be slightly larger than the majority of the full-length protein (referred to as high-migrating [hm] TLR9; Ewald et al., 2008). Treatment with baflomycinA1, an inhibitor of the vacuolar ATPase which blocks acid-dependent protease activity, prevents receptor proteolysis and results in the accumulation of hmTLR9 (Fig. 1 A; Ewald et al., 2008). It is of note that treatment with E64d (Fig. 1 B) or z-FA-FMK (Fig. 2 A) resulted in a moderate accumulation of hmTLR9, although

not to the degree observed upon baflomycinA1 treatment (Fig. 1 B; Ewald et al., 2008). The partial stabilization of hmTLR9 and formation of the untrimmed C-terminal fragments in the presence of cathepsin inhibitors are consistent with previous work suggesting that TLR9 processing may involve multiple sequential steps (Park et al., 2008). However, our results disagree with this work in one important respect: we do not observe that TLR9 processing is mediated entirely by cathepsins. Rather, the first step, performed by an unidentified protease (or proteases), results in removal of the majority of the ectodomain followed by secondary trimming of the exposed N termini, which is entirely cathepsin dependent (Fig. 1 D).

To determine whether cathepsin-mediated trimming has functional relevance for TLR9, RAW cells were treated with inhibitors before stimulation and TNF production was measured by intracellular cytokine staining. At lower concentrations of ligand, the TLR9 response to CpG could be largely blocked by pretreatment with E64d and z-FA-FMK or a combination of three individual cathepsin inhibitors; however, this inhibition was never entirely complete (Fig. 1 C and Fig. S2). The increase of the amount of ligand to 1 μ M or greater was able to overcome treatment with cathepsin inhibitors, perhaps explaining some of the discrepancy between previous studies, which conflict as to whether inhibition of cathepsins is sufficient to block TLR9 signaling (Ewald et al., 2008; Park et al., 2008). In previous studies, we and others have shown that individual cathepsin inhibitors are not sufficient to block TLR9 proteolysis (Ewald et al., 2008; Park et al., 2008), although one group has reported that combined inhibition of ctsS and ctsL appears to have a significant effect on trimming (Park et al., 2008). Collectively, we interpret these data to indicate that TLR9 trimming is a result of the redundant activities of multiple cathepsins.

AEP and cathepsins can both perform the first cleavage event in TLR9 processing

Based on the finding that broad-spectrum inhibitors failed to block the primary TLR9 cleavage event, we hypothesized that this first step in TLR9 cleavage was mediated either by a

novel protease (or proteases) or by the redundant activities of multiple proteases belonging to different families (families that were not cross-inhibited by the broad spectrum inhibitors we tested). To test the first possibility, we conducted a protease inhibitor screen using a library of \sim 1,500 compounds designed to target cysteine and serine proteases with the goal of identifying compounds that blocked TLR9 responses to CpG. Although this approach revealed several novel compounds that were able to block TLR9 signaling, subsequent analysis of TLR9 processing indicated that all of these compounds blocked cathepsin-mediated trimming rather than the primary cleavage event (unpublished data).

Based on these results, we decided to examine the possibility that the initial processing event was a result of the redundant or overlapping activities of multiple proteases belonging to different families. As a starting point, we opted to use mouse embryonic fibroblasts (MEFs) because these cells are less proteolytically complex than macrophages but can still cleave TLR9 efficiently once they have been transduced with Unc93b1, an integral membrane protein required for ER export and signaling of nucleic acid-sensing TLRs (Tabeta et al., 2006; Brinkmann et al., 2007; Ewald et al., 2008). Because cathepsins had already been implicated in TLR9 processing, we began by treating MEFs stably expressing TLR9 and Unc93b1 (Unc93b1-TLR9-MEF) with cathepsin inhibitors together with additional inhibitors. Analysis of TLR9 cleavage by pulse-chase revealed that the combination of LI-1 and z-FA-FMK was sufficient to block TLR9 cleavage to an extent equivalent to treatment with baflomycin A1 (Fig. 2 A compared with Fig. 1 A). In contrast, combining z-FA-FMK with pepstatin A and leupeptin did not block the initial cleavage event but only resulted in secondary trimming, similar to treatment with cathepsin inhibitors alone. As observed in TLR9-RAW cells, TLR9 cleavage was unaffected in Unc93b1-TLR9-MEF cells treated with LI-1 alone (Fig. 2 B). Importantly, the combination of z-FA-FMK and LI-1 was also sufficient to entirely block receptor proteolysis in TLR9-RAW cells, indicating that similar proteolytic events occur in both cell types (Fig. 2 B).

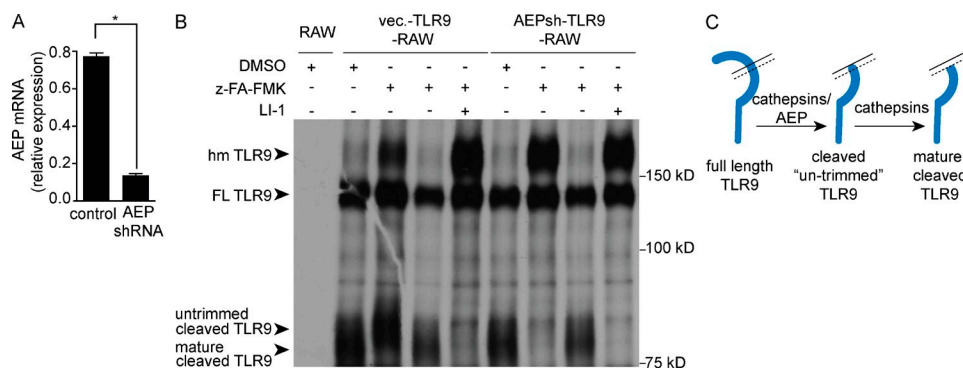


Figure 3. In the absence of AEP, TLR9 cleavage in macrophages is entirely cathepsin dependent. (A) Quantitative RT-PCR analysis of AEP transcript levels in TLR9-RAW cells transduced with an shRNA construct targeting AEP (AEP-shRNA) or vector control. AEP levels were normalized to rps17 expression. Error bars represent standard deviation. * represents $P \leq 0.001$ based on Student's *t* test. (B) TLR9 cleavage in the cells described in A as analyzed by pulse-chase analysis in the presence of indicated protease inhibitors (z-FA-FMK; LI-1) or DMSO (as vehicle control). All data are representative of two experiments. (C) Schematic illustrating the overlapping roles of AEP and cathepsins in the initial removal of the TLR9 ectodomain.

To ensure that our protease inhibitor conditions were efficient as well as specific, we used activity-based probes to detect active proteases in treated or untreated cells. Lysates of RAW cells pretreated with z-FA-FMK or LI-1 were incubated with activity-based probes DCG-04 (a biotinylated probe built on the E64d structure) or BODIPY-conjugated LI-1 (BODIPY-LI-1) to detect any cathepsins or AEP that remained unblocked after treatment (Greenbaum et al., 2000; Lee and Bogyo, 2010). Importantly, pretreatment with z-FA-FMK completely blocked cathepsin activity (Fig. 2 C, top), and pretreatment with LI-1 completely blocked AEP activity (Fig. 2 C, bottom, LI-1 lane). Furthermore, this assay revealed that cells treated with cathepsin inhibitors maintained AEP activity (Fig. 2 C, bottom, z-FA-FMK lane) and vice versa (Fig. 2 C, top, LI-1 lane), verifying, as previously reported, that these inhibitors do not cross react (Lee and Bogyo, 2010).

Consistent with the biochemical data, treatment with z-FA-FMK and LI-1 reduced TNF production in response to CpG DNA to levels comparable to unstimulated cells, whereas treatment with LI-1 alone had no effect on signaling (Fig. 2 D and Fig. S3). Notably, this effect on signaling could be overcome by treatment with very high concentrations of ligand ($>5\ \mu\text{M}$; not depicted). This observation may be the result of low levels of residual protease activity, suboptimal signaling from untrimmed or unprocessed TLRs, or TLR9 that was processed before inhibitor treatment. We have determined that the cleaved form of TLR9 is extremely stable; pulse-chase analysis indicates it remains detectable after 12 h of chase (unpublished data). However, it is unlikely that the large concentrations of ligand required to overcome inhibitor treatment are physiologically relevant.

In the absence of AEP, TLR9 processing is entirely cathepsin dependent

The data presented thus far suggest that cathepsins and AEP play a functionally redundant role in the first step of TLR9 proteolysis. In the absence of AEP activity, cathepsins can compensate for the initial processing event as well as trim the processed receptor, resulting in the fully mature form of TLR9. In contrast, when cathepsin activity is blocked, the initial processing event is still performed by AEP; however, the cleaved receptor can no longer be trimmed, which results in a slightly larger cleaved form of the receptor and impaired signaling (Fig. 3 C, model).

This model predicts that in the absence of AEP, TLR9 processing should be entirely cathepsin dependent. To test this possibility, we stably transduced TLR9-RAW cells with retroviruses encoding a short hairpin RNA (shRNA) targeting AEP (AEPsh-TLR9-RAW). AEP transcript levels in AEPsh-TLR9-RAW cells were reduced to nearly 25% of the levels normally seen in vector-transduced TLR9-RAW cells (Fig. 3 A). Pulse-chase analysis revealed that TLR9 processing in AEP knockdown cells was intact, which is consistent with our observation that LI-1 treatment alone does not impair TLR9 processing (Fig. 2 B). However, treatment with z-FA-FMK was now sufficient to completely block the

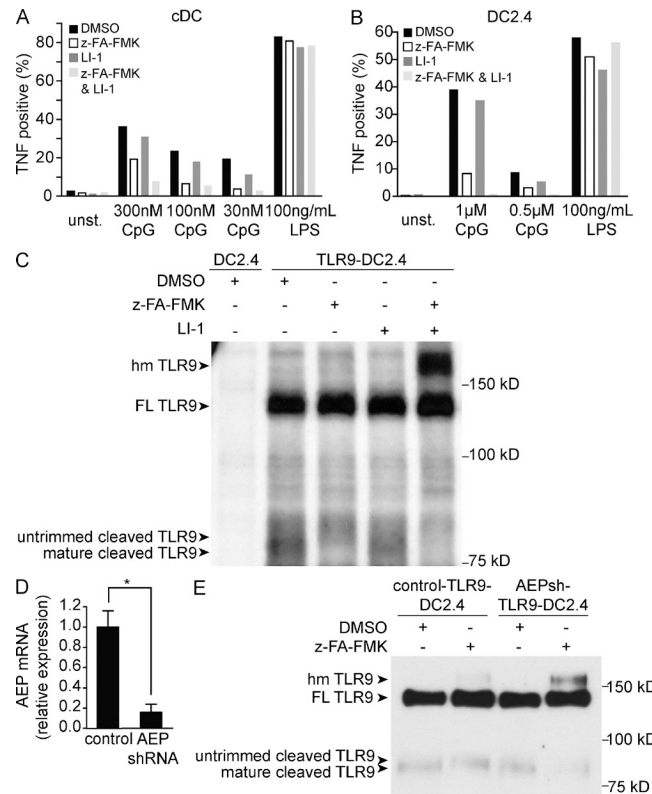


Figure 4. TLR9 signaling and cleavage in DCs requires AEP and cathepsins. (A and B) TNF production by GM-CSF-derived DCs (A) or DC2.4 cells (B) was monitored by intracellular cytokine staining as described in Fig. 1. Representative FACS plots are shown in Fig. S4. Data are representative of three experiments. (C) TLR9 cleavage in TLR9-DC2.4 cells or DC2.4 cells was monitored by pulse-chase analysis as described in Materials and methods. Data are representative of four experiments. (D) Quantitative RT-PCR analysis of AEP transcript levels in TLR9-DC2.4 cells transduced with the AEP shRNA (AEP-shRNA) or an unrelated gene product (control). AEP levels were normalized to *rps17* expression. Error bars represent standard deviation. * represents $P \leq 0.005$ based on Student's *t* test. (E) TLR9 cleavage in the cells described in D visualized by immunoblot after immunoprecipitation after 14 h of z-FA-FMK or DMSO treatment. Data in E are representative of three experiments.

appearance of cleaved TLR9 and allow hmTLR9 to accumulate (Fig. 3 B). In contrast, z-FA-FMK treatment only prevented receptor trimming in the vector-transduced control cells (Fig. 3 B, vec.-TLR9-RAW). We interpret these results to indicate that cathepsins are sufficient to carry out both TLR9 processing steps in the absence of AEP (Fig. 3 C).

Cathepsin activity is required for optimal TLR9 processing and function in DCs

A recent paper from Sepulveda et al. (2009) has described a significant defect in TLR9 processing and signaling in AEP-deficient DCs. This role for AEP in TLR9 function was only observed in DCs. Although our results with macrophages and fibroblasts suggest that cathepsins can mediate TLR9 processing in the absence of AEP, it is possible that the proteases required for TLR9 processing in DCs are distinct from those in

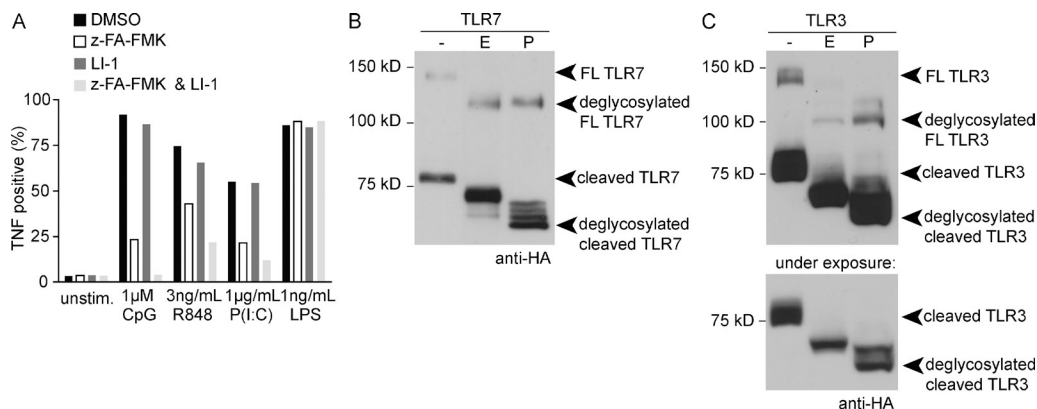


Figure 5. TLR7 and TLR3 are regulated by receptor proteolysis. (A) TNF production by RAW cells in response to TLR9, TLR3, and TLR7 ligands was measured by intracellular cytokine staining as described in Fig. 1. Representative FACS plots are shown in Fig. S6. (B and C) TLR7 (B) and TLR3 (C) are cleaved after trafficking through the Golgi. TLR7-RAW (B) or TLR3-RAW (C) cell immunoprecipitates were treated with Endo H (E), PNGase (P), or no enzyme control (–) to assess glycosylation status by anti-HA Western blotting. The bottom panel in C is a shorter exposure of the TLR3 cleaved product. All data are representative of three experiments.

other cell types. To address this possibility, we first examined the effect of cathepsin and AEP inhibitors on TLR9 signaling in DCs derived from bone marrow with GM-CSF or in the DC cell line DC2.4. Similar to our experiments with macrophages (Fig. 2), we observed that TNF production in response to CpG was inhibited by z-FA-FMK (Fig. 4, A and B; and Fig. S4). Inhibition of AEP did result in slightly reduced TLR9 signaling, suggesting that AEP may play a more prevalent role in TLR9 processing in DCs than in macrophages and fibroblasts. However, TNF production was more effectively blocked by z-FA-FMK than by LI-1. Combined treatment with z-FA-FMK and LI-1 resulted in greater inhibition of TLR9 signaling compared with z-FA-FMK alone (Fig. 4, A and B).

To examine more directly the relative contribution of these proteases on TLR9 cleavage in DCs, we generated DC2.4 cells stably expressing TLR9-HA (TLR9-DC2.4). Similar to our results in macrophages and fibroblasts, z-FA-FMK treatment inhibited only the second proteolytic event (Fig. 4 C). Inhibition of AEP alone had no detectable effect on processing. However, inhibition of AEP and cathepsins in combination blocked processing completely and resulted in accumulation of the high migrating form of TLR9 (hmTLR9; Fig. 4 C). As a final approach, we knocked down AEP in TLR9-DC2.4 cells (AEPsh-TLR9-DC2.4) using the same shRNA as that described earlier (Fig. 4 D). The combination of cathepsin inhibition and AEP knockdown allowed the unprocessed hmTLR9 band to accumulate and reduced the amount of cleaved TLR9 (Fig. 4 E). TLR9 signaling correlated with these biochemical data; AEP knockdown cells responded normally to CpG DNA but were more sensitive to cathepsin inhibitors than control cells (Fig. S5).

Collectively, these results indicate that cathepsins play a prominent role in TLR9 proteolysis in DCs as well as in macrophages. The role for AEP appears to be largely redundant with cathepsins, although our signaling experiments do

support a potentially greater role for AEP in DCs than in other cell types. It is possible that our inability to resolve a dominant role for AEP in TLR9 processing is a result of our use of pharmacological inhibition of AEP which is unlikely to be as complete as a genetic deficiency in AEP (Sepulveda et al., 2009). However, our analysis of AEP knockdown cells also implicates cathepsins in TLR9 processing in DCs. This is consistent with the observation that AEP-independent proteolysis of TLR9 occurs after DC activation (Sepulveda et al., 2009). AEP has also been shown to contribute to the processing of procathepsins, so another explanation for the discrepancy in protease bias for TLR9 maturation is that AEP-deficient cells may have reduced activity of other proteases, most notably cathepsins (Shirahama-Noda et al., 2003; Maehr et al., 2005). In any case, our analysis of signaling and receptor processing support a role for both cathepsins and AEP in TLR9 proteolysis in all cell types tested. It remains formally possible that certain cell types rely more heavily on subsets of these proteases, especially considering reports of significantly distinct protease complexity between cell types (Delamarre et al., 2005). Additional analysis of purified populations of cells may address this possibility.

TLR3 and TLR7 are processed and require cathepsin activity for optimal signaling

If receptor proteolysis represents a strategy to avoid recognition of self-nucleic acids, then one might expect nucleic acid-sensing TLRs other than TLR9 to be similarly regulated. Based on our findings that cathepsins and AEP are required for TLR9 processing, we examined the role of these proteases in the activation of TLR3 and TLR7. First, we measured TNF produced in response to the TLR7 ligand R848 or the TLR3 ligand poly(I:C) in RAW cells pretreated with z-FA-FMK, LI-1, or both inhibitors. Similar to our results with TLR9, TLR7 and TLR3 responses were impaired in cells treated with z-FA-FMK or z-FA-FMK combined with LI-1

(Fig. 5 A and Fig. S6). Treatment with LI-1 alone had little effect on TLR7 or TLR3 responses.

To examine TLR7 and TLR3 processing directly, we generated RAW cells stably expressing TLR7 or TLR3 bearing C-terminal HA tags. A cleaved form of each receptor was detectable by immunoblot (Fig. 5, B and C). Moreover, the sensitivity of the N-linked glycans to endoglycosidase H (Endo H) and PNGase is consistent with TLR3 and TLR7 trafficking similarly to TLR9. Full-length TLR7 and full-length TLR3 were Endo H sensitive, indicating that these forms of the proteins were localized in the ER (Fig. 5, B and C). In contrast, the cleaved forms of TLR7 and TLR3 were mostly Endo H resistant when compared with treatment with PNGase, indicating that they have trafficked through the Golgi en route to the endolysosome (Fig. 5, B and C). In sum, these data suggest that TLR7 and TLR3 are proteolytically processed in a manner similar to that of TLR9. Furthermore, proteolysis is required for the optimal signaling of these receptors.

In previous work, we put forth the hypothesis that proteolytic processing is required to limit TLR9 activation to the endolysosomal compartments where nucleic acids are more likely to be foreign in origin than host derived (Ewald et al., 2008). Sequence comparison of known vertebrate TLRs reveals that TLR7, TLR8, and TLR9 represent a family of closely related TLRs that appear to have bifurcated from other TLRs on a branch that also includes the TLR3 family (Roach et al., 2005). The findings presented in this paper suggest that receptor proteolysis is a regulatory mechanism that may have evolved alongside the ability to recognize nucleic acids as a signature of infection.

Based on the accepted role that TLR7 and TLR9 play in contributing to lupus, arthritis, and psoriasis, it is reasonable that these receptors would be regulated in a similar manner. However, the finding that TLR3 is proteolytically processed, and that processing is required for an optimal response to poly(I:C), is rather surprising as activation of TLR3 by self-nucleic acids has not been implicated in any autoimmune diseases. Structural studies of the TLR3 ectodomain bound to poly(I:C) indicate that a C-terminal cleavage product of TLR3 would contain residues implicated in direct interaction between the two TLR3 molecules within the dimer as well as the lateral face (leucine-rich repeat [LRR] 19–LRR21) required for ligand binding (Bell et al., 2006; Liu et al., 2008). However, a putative ligand-binding site composed of basic residues within LRR1 and LRR3 would be removed upon proteolysis (Bell et al., 2006; Liu et al., 2008; Botos et al., 2009). Interestingly, mutational analysis of the TLR9 N terminus indicates that an analogous positively charged region may also be required for receptor activation (Peter et al., 2009). It certainly remains possible that the N terminus plays an important role in the biology of these receptors before cleavage.

It is still unclear precisely how receptor proteolysis permits TLR activation. A study using fluorescently labeled TLR9 molecules to monitor protein interactions suggests that ligand binding by the TLR9 dimer induces a conformational change that brings the TIR domains in close proximity, enabling

signal transduction (Latz et al., 2007). Proteolysis may be required for this conformational shift in dimer structure. Alternatively, receptor cleavage may lead to altered affinity for ligand, which could also increase the likelihood of receptor activation. Although proteolysis seems to be an important requirement for all nucleic acid–sensing TLRs, whether the mechanisms that dictate this requirement are similar between TLR family members is not yet clear. Future studies focusing on the structural significance of receptor proteolysis and how this event contributes to the orchestration of ligand binding, dimerization, and functional nucleic acid sensing will be of great value.

Finally, it is not obvious why so many proteases are able to process TLR9. The experiments presented in this paper indicate that the use of AEP and cathepsins is largely conserved across cell types, although the role that these proteases play is not entirely overlapping. One possible explanation for the observed redundancy is that the region subject to proteolysis is unstructured and easily accessible. The ectodomains of TLR9, TLR7, and TLR3 all contain inserts or nonconserved regions between LRRs. For example, TLR9 contains a large nonconserved loop between LRR14 and LRR15 that is susceptible to cathepsin-mediated proteolysis and contains at least two potential AEP consensus sites (Park et al., 2008; Sepulveda et al., 2009). It may be that the initial site of proteolysis is not particularly important for receptor function. Instead, any cleavage event within the unstructured loop may be sufficient to allow cathepsins to trim the receptor to an optimal size for signaling. This mechanism could also allow for increased complexity in the number of proteases able to make the initial cut in TLR9.

Allowing flexibility in the types of proteases that can cleave the receptor has several perceivable advantages. Such flexibility may ensure that TLR9 can be activated across cell types expressing different protease repertoires or may allow the receptor to be activated throughout the endosomal system as the pool of active proteases changes. For example, it has been proposed that differential cytokine production in response to TLR9 ligands is compartment specific; activation from one class of endosome leads to type I interferon production, whereas activation in a distinct pool of endosomes results in a proinflammatory signature (Honda et al., 2005; Guiducci et al., 2006; Sasai et al., 2010). Whether the proteolytic constituents of these compartments play a role in establishing these differences or other instances of differential signaling is an interesting possibility that requires further attention.

MATERIALS AND METHODS

Reagents. All chemicals and reagents, unless noted otherwise, were purchased from Thermo Fisher Scientific. Anti-HA (Clone 3F10) matrix was purchased from Roche. CpG oligonucleotides (TCCATGACGTTCCCT-GACGTT) with phosphorothioate linkages were purchased from Invitrogen. LPS, R848, and P(I:C) were purchased from InvivoGen. All antibodies for flow cytometry and ELISAs were purchased from eBioscience. Anti-HA (Roche) and goat anti–rat HRP (GE Healthcare) antibodies were used for immunoblotting. DMSO, z-FA-FMK, baflomycin A1, pepstatin A, and leupeptin (Sigma-Aldrich); ctsL inhibitor I (Z-Phe-Phe-CH2F), ctsB inhibitor

(Me047), ctsS inhibitor (-Phe-Leu-COCHO-H₂O; EMD); and LI-1, DCG-04, and BODIPY-LI-1 (synthesized by J. Lee) were used in pulse-chase assays and signaling assays at the indicated concentrations.

Cell lines, plasmids, tissue culture, and mice. RAW264 cells were purchased from American Type Culture Collection. DC2.4 cells were provided by L. Coscoy (University of California, Berkeley, Berkeley, CA) and cultured in RPMI supplemented with 10% FCS, L-glutamine, penicillin/streptomycin, sodium pyruvate, and HEPES (all obtained from Invitrogen). MEFs were generated as previously described and cultured in DME supplemented with penicillin/streptomycin, L-glutamine, sodium pyruvate, and Hepes (Barton et al., 2006). Unless otherwise noted, stable lines were generated by transducing cells with MSCV2.2 retroviruses encoding the target cDNA. When combined with the LMP knockdown vector, TLR9HA transduction of DC2.4 was achieved using pQCXIH. For RAW-TLR9, RAW-TLR7, RAW-hTLR3, and TLR9-Unc93b1-MEF cells, cDNA encoding the HA epitope was inserted at the 3' end of each TLR.

C57BL/6 mice were purchased from The Jackson Laboratory. All mice were housed within the animal facilities at the University of California at Berkeley or University of California according to Institutional Animal Care and Use Committee guidelines. Animal work was conducted according to University of California Berkeley Animal Care and Use Committee guidelines. Bone marrow-derived conventional DCs were differentiated, as previously described, in RPMI supplemented with GM-CSF containing supernatant.

Immunoprecipitation and Western blot analyses. Cells were lysed in RIPA buffer (50 mM Tris, pH 8, 150 mM NaCl, 1% NP-40, 0.5% sodium deoxycholate, and 0.1% SDS) supplemented with complete protease inhibitor cocktail (Roche). After incubation on ice, lysates were cleared of insoluble material by centrifugation. For immunoprecipitations, lysates were incubated with anti-HA matrix and precipitated proteins were separated by SDS-PAGE and transferred to Immobilon PVDF membrane (Millipore). Deglycosylation kits (New England Biolabs, Inc.) were performed according to the manufacturer's instructions. Membranes were probed with the indicated antibodies and developed by ECL chemiluminescence (Thermo Fisher Scientific).

Pulse-chase analysis. Cells were starved for 1 h in cysteine/methionine-free media, and then pulsed with 0.25 mCi ³⁵S-cysteine/methionine (PerkinElmer). After a 60-min pulse, cells were washed and cultured in 5 ml of chase media with a 10,000-fold molar excess of L-cysteine or L-methionine or harvested as the zero time point. Time points were harvested after 5 h as follows: cells were washed in 3 mL PBS and lysed in 1 mL RIPA plus protease inhibitor cocktail. Protease inhibitors were added in the pulse and chase medias at the following concentrations: 50 μM E64d, 10 μM z-FA-FMK, 50 μM LI-1, 100 μM pepstatin A, 100 μM leupeptin, and 10 μg/ml bafilomycin A1.

Measure of protease inhibitor efficiency. 10⁶ RAW cells were plated and incubated for 1 h with 10 μM or 1 μM z-FA-FMK, 50 μM E64d, 50 μM LI-1, and DMSO. Cells were washed in PBS and lysed in 50 mM citrate buffer (pH 4.5, 1% CHAPS, 0.5% Triton X-100, and 5 mM DTT) followed by incubation with 1 μM DCG-04 or BODIPY-LI-1 for 30 min. Protein concentration was determined by BSA, and 25 μg of protein lysate was separated by SDS-PAGE and transferred to Immobilon PVDF membrane (Millipore) or imaged by LI-CORE (LI-COR Biosciences). Membranes were probed with streptavidin-HRP (Invitrogen) and developed by ECL chemiluminescence (Thermo Fisher Scientific).

Intracellular cytokine staining. RAW cells or DCs were plated at 2.5 × 10⁵ on 96-well plates and allowed to settle for 1–3 h. Cells were incubated with inhibitors for 10 h at the following concentrations: 50 μM E64d, 10 μM z-FA-FMK, 30 μM ctsB inhibitor, 2 μM ctsS inhibitor, 10 μM ctsL inhibitor, or 50 μM LI-1. After 4 h of stimulation with indicated TLR ligands in the presence of brefeldin A, cells were harvested and stained with a fixation and permeabilization kit (eBioscience) according to the manufacturer's protocol.

DCs were stained with anti-CD11b (M1/70), anti-CD11c (N418), anti-TNF (MP6-XT22; all obtained from eBioscience), and anti-CD16/CD32 antibody (2.4G2; University of California, San Francisco Monoclonal Antibody Core) as indicated.

AEP knockdown and quantitative real-time RT-PCR. Sense and antisense oligonucleotides targeting AEP (sense sequence: 5'-CCGAGAT-CATGTCTTCATTTAC-3') were cloned into the LMP retroviral vector (Thermo Fisher Scientific) according to the manufacturer's instructions. Cells were carried in 4 μg/ml puromycin. Constructs were introduced into RAW cells or DC2.4 cells by retroviral transduction and knockdown was assessed by quantitative real-time RT-PCR. In brief, RNA was isolated using TRIzol plus RNA Purification System (Invitrogen). Gene-specific transcript levels were normalized to RPS17 mRNA. The following primers were used: AEP, 5'-GGAAGCTGCTGAGAACCAAC-3' and 5'-TGTG-AGCATGGTCCTCTCTG-3'; RPS17, 5'-CGCCATTATCCCCAG-CAAG-3' and 5'-TGTGGGATCCACCTCAATG-3'.

Online supplemental material. Fig. S1 shows deglycosylated TLR9 after treatment with protease inhibitors. Figs. S2–S4 and S6 show representative FACS plots for bar graphs depicted in Figs. 1–2 and 4–5, respectively. Fig. S5 shows representative signaling data for the AEP knockdown DC2.4 cells described in Fig. 5. Online supplemental material is available at <http://www.jem.org/cgi/content/full/jem.20100682/DC1>.

We thank R. Vance and Barton, Vance, and Boygo laboratory members for helpful discussions; and E. Ponder and V. Albow for technical assistance.

This work was supported by grants from the National Institutes of Health (AI0172429 to G.M. Barton; EB005011 to M. Boygo), the Lupus Research Institute (G.M. Barton), and the Irvington Institute Fellowship Program of the Cancer Research Institute (A. Engel).

The authors declare no competing interests.

Submitted: 7 April 2010

Accepted: 10 February 2011

REFERENCES

Asagiri, M., T. Hirai, T. Kunigami, S. Kamano, H.-J. Gober, K. Okamoto, K. Nishikawa, E. Latz, D.T. Golenbock, K. Aoki, et al. 2008. Cathepsin K-dependent toll-like receptor 9 signaling revealed in experimental arthritis. *Science*. 319:624–627. doi:10.1126/science.1150110

Barton, G.M., J.C. Kagan, and R. Medzhitov. 2006. Intracellular localization of Toll-like receptor 9 prevents recognition of self DNA but facilitates access to viral DNA. *Nat. Immunol.* 7:49–56. doi:10.1038/ni1280

Bell, J.K., J. Askins, P.R. Hall, D.R. Davies, and D.M. Segal. 2006. The dsRNA binding site of human Toll-like receptor 3. *Proc. Natl. Acad. Sci. USA*. 103:8792–8797. doi:10.1073/pnas.0603245103

Botos, I., L. Liu, Y. Wang, D.M. Segal, and D.R. Davies. 2009. The toll-like receptor 3:dsRNA signaling complex. *Biochim. Biophys. Acta*. 1789:667–674.

Brinkmann, M.M., E. Spooner, K. Hoebe, B. Beutler, H.L. Ploegh, and Y.-M. Kim. 2007. The interaction between the ER membrane protein UNC93B and TLR3, 7, and 9 is crucial for TLR signaling. *J. Cell Biol.* 177:265–275. doi:10.1083/jcb.200612056

Delamarre, L., M. Pack, H. Chang, I. Mellman, and E.S. Trombetta. 2005. Differential lysosomal proteolysis in antigen-presenting cells determines antigen fate. *Science*. 307:1630–1634. doi:10.1126/science.1108003

Ewald, S.E., B.L. Lee, L. Lau, K.E. Wickliffe, G.-P. Shi, H.A. Chapman, and G.M. Barton. 2008. The ectodomain of Toll-like receptor 9 is cleaved to generate a functional receptor. *Nature*. 456:658–662. doi:10.1038/nature07405

Greenbaum, D., K.F. Medzhitov, A. Burlingame, and M. Boygo. 2000. Epoxide electrophiles as activity-dependent cysteine protease profiling and discovery tools. *Chem. Biol.* 7:569–581. doi:10.1016/S1074-5521(00)00014-4

Guiducci, C., G. Ott, J.H. Chan, E. Damon, C. Calacsan, T. Matray, K.D. Lee, R.L. Coffman, and F.J. Barrat. 2006. Properties regulating the nature of

the plasmacytoid dendritic cell response to Toll-like receptor 9 activation. *J. Exp. Med.* 203:1999–2008. doi:10.1084/jem.20060401

Honda, K., Y. Ohba, H. Yanai, H. Negishi, T. Mizutani, A. Takaoka, C. Taya, and T. Taniguchi. 2005. Spatiotemporal regulation of MyD88-IRF-7 signalling for robust type-I interferon induction. *Nature*. 434:1035–1040. doi:10.1038/nature03547

Kim, Y.M., M.M. Brinkmann, M.E. Paquet, and H.L. Ploegh. 2008. UNC93B1 delivers nucleotide-sensing toll-like receptors to endolysosomes. *Nature*. 452:234–238. doi:10.1038/nature06726

Krieg, A.M., and J. Vollmer. 2007. Toll-like receptors 7, 8, and 9: linking innate immunity to autoimmunity. *Immunol. Rev.* 220:251–269. doi:10.1111/j.1600-065X.2007.00572.x

Latz, E., A. Verma, A. Visintin, M. Gong, C.M. Sirois, D.C. Klein, B.G. Monks, C.J. McKnight, M.S. Lamphier, W.P. Duprex, et al. 2007. Ligand-induced conformational changes allosterically activate Toll-like receptor 9. *Nat. Immunol.* 8:772–779. doi:10.1038/ni1479

Lee, J., and M. Bogyo. 2010. Development of near-infrared fluorophore (NIRF)-labeled activity-based probes for in vivo imaging of legumain. *ACS Chem. Biol.* 5:233–243. doi:10.1021/cb900232a

Liu, L., I. Botos, Y. Wang, J.N. Leonard, J. Shiloach, D.M. Segal, and D.R. Davies. 2008. Structural basis of toll-like receptor 3 signaling with double-stranded RNA. *Science*. 320:379–381. doi:10.1126/science.1155406

Maehr, R., H.C. Hang, J.D. Mintern, Y.M. Kim, A. Cuvillier, M. Nishimura, K. Yamada, K. Shirahama-Noda, I. Hara-Nishimura, and H.L. Ploegh. 2005. Asparagine endopeptidase is not essential for class II MHC antigen presentation but is required for processing of cathepsin L in mice. *J. Immunol.* 174:7066–7074.

Matsumoto, F., S. Saitoh, R. Fukui, T. Kobayashi, N. Tanimura, K. Konno, Y. Kusumoto, S. Akashi-Takamura, and K. Miyake. 2008. Cathepsins are required for Toll-like receptor 9 responses. *Biochem. Biophys. Res. Commun.* 367:693–699. doi:10.1016/j.bbrc.2007.12.130

Park, B., M.M. Brinkmann, E. Spooner, C.C. Lee, Y.-M. Kim, and H.L. Ploegh. 2008. Proteolytic cleavage in an endolysosomal compartment is required for activation of Toll-like receptor 9. *Nat. Immunol.* 9:1407–1414. doi:10.1038/ni.1669

Peter, M.E., A.V. Kubarenko, A.N.R. Weber, and A.H. Dalpke. 2009. Identification of an N-terminal recognition site in TLR9 that contributes to CpG-DNA-mediated receptor activation. *J. Immunol.* 182:7690–7697. doi:10.4049/jimmunol.0900819

Roach, J.C., G. Glusman, L. Rowen, A. Kaur, M.K. Purcell, K.D. Smith, L.E. Hood, and A. Aderem. 2005. The evolution of vertebrate Toll-like receptors. *Proc. Natl. Acad. Sci. USA*. 102:9577–9582. doi:10.1073/pnas.0502272102

Rudensky, A., and C. Beers. 2006. Lysosomal cysteine proteases and antigen presentation. *Ernst Schering Res. Found. Workshop*. 56:81–95. doi:10.1007/3-540-37673-9_5

Sasai, M., M.M. Linehan, and A. Iwasaki. 2010. Bifurcation of Toll-like receptor 9 signaling by adaptor protein 3. *Science*. 329:1530–1534. doi:10.1126/science.1187029

Sepulveda, F.E., S. Maschalidi, R. Colisson, L. Heslop, C. Ghirelli, E. Sakka, A.-M. Lennon-Duménil, S. Amigorena, L. Cabanie, and B. Manoury. 2009. Critical role for asparagine endopeptidase in endocytic Toll-like receptor signaling in dendritic cells. *Immunity*. 31:737–748. doi:10.1016/j.jimmuni.2009.09.013

Shirahama-Noda, K., A. Yamamoto, K. Sugihara, N. Hashimoto, M. Asano, M. Nishimura, and I. Hara-Nishimura. 2003. Biosynthetic processing of cathepsins and lysosomal degradation are abolished in asparaginyl endopeptidase-deficient mice. *J. Biol. Chem.* 278:33194–33199. doi:10.1074/jbc.M302742200

Tabeta, K., K. Hoebe, E.M. Janssen, X. Du, P. Georgel, K. Crozat, S. Mudd, N. Mann, S. Sovath, J. Goode, et al. 2006. The Unc93b1 mutation 3d disrupts exogenous antigen presentation and signaling via Toll-like receptors 3, 7 and 9. *Nat. Immunol.* 7:156–164. doi:10.1038/ni1297